THE JOURNAL OF PHYSICAL CHEMISTRY Letters

Cite This: J. Phys. Chem. Lett. 2018, 9, 4679−4685

Letter

pubs.acs.org/JPCL

# Small Unnatural Amino Acid Carried Raman Tag for Molecular Imaging of Genetically Targeted Proteins

Jing Zhang,[†,‡,#] Shuai Yan,[†,‡,#] Zhiyong He,[§,#] Cong Ding,[§,#] Tianxing Zhai,[†] Yage Chen,[†,‡] Haozheng Li,[†,‡] Guang Yang,[†,‡] Xiang Zhou,[§] and Ping Wang*[,†,‡]

[†]Britton Chance Center for Biomedical Photonics, Wuhan National Laboratory for Optoelectronics−Huazhong University of Science and Technology, Wuhan, Hubei 430074, China

[‡]MoE Key Laboratory for Biomedical Photonics, Collaborative Innovation Center for Biomedical Engineering, School of Engineering Sciences, Huazhong University of Science and Technology, Wuhan, Hubei 430074, China

[§]College of Chemistry and Molecular Sciences, Key Laboratory of Biomedical Polymers of the Ministry of Education, Wuhan University, Wuhan, Hubei 430072, China

Supporting Information

**ABSTRACT:** Raman has been implemented to image biological systems for decades. However, Raman microscopy along with Raman probes is restricted to image metabolites or a few intracellular organelles so far and lacks genetic specificity for imaging proteins of interest, which significantly hinders their application. Here, we report the Raman spectra-based protein imaging method, which incorporates a small phenyl ring enhanced Raman tag (total of ∼0.55 kDa) with a single unnatural amino acid (UAA) to genetically label specific proteins. We further demonstrate hyperspectral stimulated Raman scattering (SRS) imaging of the Histone3.3 protein in the nucleus, Sec61$\beta$ protein in the endoplasmic reticulum of HeLa cells, and Huntingtin protein Htt74Q in mutant huntingtin-induced cells. Genetic encoding of a small, stable, sensitive, and narrow-band Raman tag took one key step forward to enable SRS or Raman imaging of specific proteins and could further facilitate quantitative Raman spectra-based supermultiplexing microscopy in the future.

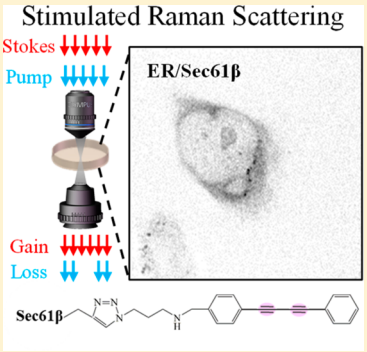




To visualize specific proteins in single cells, genetic encoding of green fluorescent protein (GFP) has been extensively used as a labeling technique that tremendously revolutionized our understanding of molecular and genetic mechanisms underlying biology.[1] Because of its excellent performance in both genetic specificity and fluorescent brightness, GFP labeling has been applied not only in mammalian cells but also in countless model organisms. However, GFP is a large protein composed of 238 amino acid residues (∼27 kDa), and either its spatial size or molecular weight may be much greater than the protein of interest, which results in unknown perturbations to native functions of the proteins at different levels in living cells.[2−4] In addition, the spectral width of fluorescence is too broad (tens of nanometers) to be applied for multicolor labeling at a time,[5] which has been a major hurdle for fluorescence-based imaging techniques.

In the most recent endeavor, the single unnatural amino acid (UAA), an analogue of pyrrolysine[6,7] (the 22nd genetically encoded amino acid) or other types of UAAs bearing strained alkyne or alkene functionalities, was successfully incorporated into a specific protein by an encoded amber codon in mRNA.[8−12] All of these tagging strategies successfully reduced the potential risks of functional and structural perturbations to proteins. However, they inevitably relied on fluorescent ligands,[2,13] immunofluorescence,[14] various dyes, and other fluorescent chemicals[15−17] as reporters to provide contrasts during imaging. In a recent advance, Wei Min and his colleagues successfully developed a powerful supermultiplex vibrational imaging technology by synthesized Manhattan Raman scattering (MARS) and carbon rainbow (Carbow) dyes with great photostability.[18−20] However, the main drawback of Raman[21,22] is that it lacks genetic specificity to identify and image distinct proteins of interest. To fill this gap, we developed a methodology for Raman tag-based protein imaging by combining advanced genetic code expansion with hyperspectral stimulated Raman scattering (SRS) microscopy.

*UAA Carried Raman Tag for SRS Imaging of a Specific Protein.* For better understanding, the concept of the amber-UAA-Raman tag system is graphically summarized in Figure 1a. To specifically incorporate a Raman tag into the protein, we purposely selected a pyrrolysine analogue, N$\varepsilon$-[(2-propynyloxy)carbonyl]-L-lysine (UAA **1**, Figure 1b), which specifically bears an alkyne (C≡C) and has been genetically encoded in *Escherichia coli*,[23] yeast,[24] mammalian cells,[25] and even animals.[26,27] With an expressed orthogonal *Methanosarcina bakeri (Mb)* pyrrolysine tRNA synthase (PylRS, encoded by *PylS*)/tRNA$_{CUA}$ (encoded by *PylT*) pair, the UAA **1** carried by

**Received:** June 25, 2018
**Accepted:** August 1, 2018
**Published:** August 1, 2018





DOI: 10.1021/acs.jpclett.8b01991
J. Phys. Chem. Lett. 2018, 9, 4679−4685

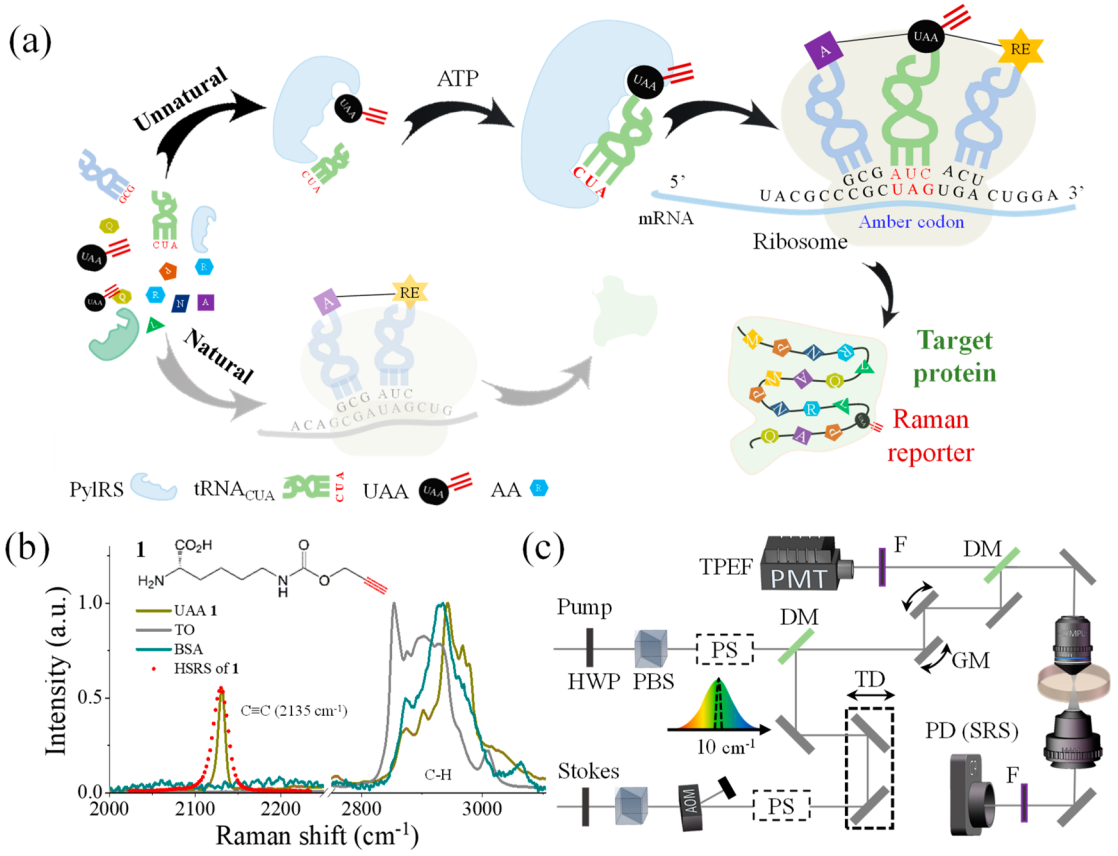


**Figure 1.** Incorporation of a Raman tag via genetic code expansion and hyperspectral SRS microscopy. (a) Schematic representation of the amber-UAA-Raman tag system for genetically targeted protein imaging. AA: amino acid; RE: release factor. (b) Chemical structure of UAA **1**, spontaneous Raman spectra of UAA **1**, TO and BSA, and SRS spectrum of UAA **1** for comparison. (c) Schematic representation of the hyperspectral SRS microscope for vibrational imaging of a genetically encoded Raman tag. PMT: photomultiplier tube; F: optical filters; DM: dichroic mirror; GM: galvanometer; PS: pulse shaper; PBS: polarization beam splitter; HWP: half-wave plate; TD: time delay; PD: photodiode; AOM: acousto-optic modulator.

the tRNA$_{CUA}$ could be directly introduced into the target protein by recognition of the amber codon (UAG) encoded in mRNA of the target protein.[28−30]

The alkyne neither exists in the natural biological system nor reacts with endogenous biomolecules.[31] As shown in Figure 1b, the stretching vibration of the C≡C bond displays a very sharp Raman peak at 2135 cm$^{-1}$ (dark yellow), which lies in the silent region of the Raman spectrum. In contrast to the combinational Raman bands observed for glyceryl trioleate (TO, an analogue of lipids) and bovine serum albumin (BSA, an analogue of protein) in the crowded C−H region, alkyne provides excellent chemical specificity with a clear spectral background for both identification and imaging.[18,32,33] In Figure 1b, we also show the SRS spectrum of UAA **1** (red dots), which is consistent with the spectrum measured by spontaneous Raman (dark yellow). Figure 1c schematically illustrates the hyperspectral SRS setup, which was employed to perform molecular imaging of Raman tags in our study (see more details of the setup in the Methods section).

*Incorporation of UAA 1 into Histone3.3-EGFP Protein via Genetic Code Expansion.* To introduce UAA **1** into a specific site in the protein of interest, we cotransfected HeLa cells with two plasmids, which expressed the orthogonal PylRS/tRNA$_{CUA}$ pair (Figure 2a(a), Note S2) and the Histone3.3-EGFP (Figure 2a(b)), respectively.[23,29] Because the eukaryotic cells lack the *PylT* gene,[7] we constructed eight copies of *PylT*, and each was driven by a U6 (RNA polymerase III) promoter.[34,35] The *PylS* gene was expressed under the chicken *β*-actin promoter for efficient and continuous expression of PylRS in cells, and mCherry (transcripted from an internal entry site (IRES2)) was used as a reporter to confirm the expression of PylRS (Figure S1(1)). In the second plasmid, we expressed Histone3.3 protein fused to EGFP, in which the codon N150 was replaced with an amber codon (*Histone3.3-EGFP-(N150TAG)*) by site-directed mutagenesis (Figure S1(2)).[34,36,37] Here, the Histone3.3-EGFP was expressed under the cytomegalovirus (CMV) promoter. The fluorescence, Western blotting, and control experiments for genetic incorporation of UAA **1** in HeLa cells are illustrated in Figure S2.

To prove our concept, we implemented a multiplex SRS microscope to image Histone3.3 protein, which was genetically targeted by UAA **1** and carried an alkyne. Figure 2b shows the two-photon excited fluorescence (TPEF) images of mCherry, which indicated the expression of PylRS in HeLa cells, and the incorporation of UAA **1** was confirmed by EGFP in the nucleus. We further performed multiplex SRS imaging of the transfected cell with Raman shift covering 2079−2191 cm$^{-1}$ (Figure 2d, total of 9 SRS images). For each SRS image, we averaged 200 times with a dwell time of 40 *μ*s for each pixel. Although the vibrational signal of alkyne was very weak, we obtained a clear SRS image of the Histone3.3 protein in the nucleus when the Raman shift was set at 2135 cm$^{-1}$. When we tuned the Raman shift to off-resonance of the alkyne, the


DOI: 10.1021/acs.jpclett.8b01991
J. Phys. Chem. Lett. 2018, 9, 4679−4685

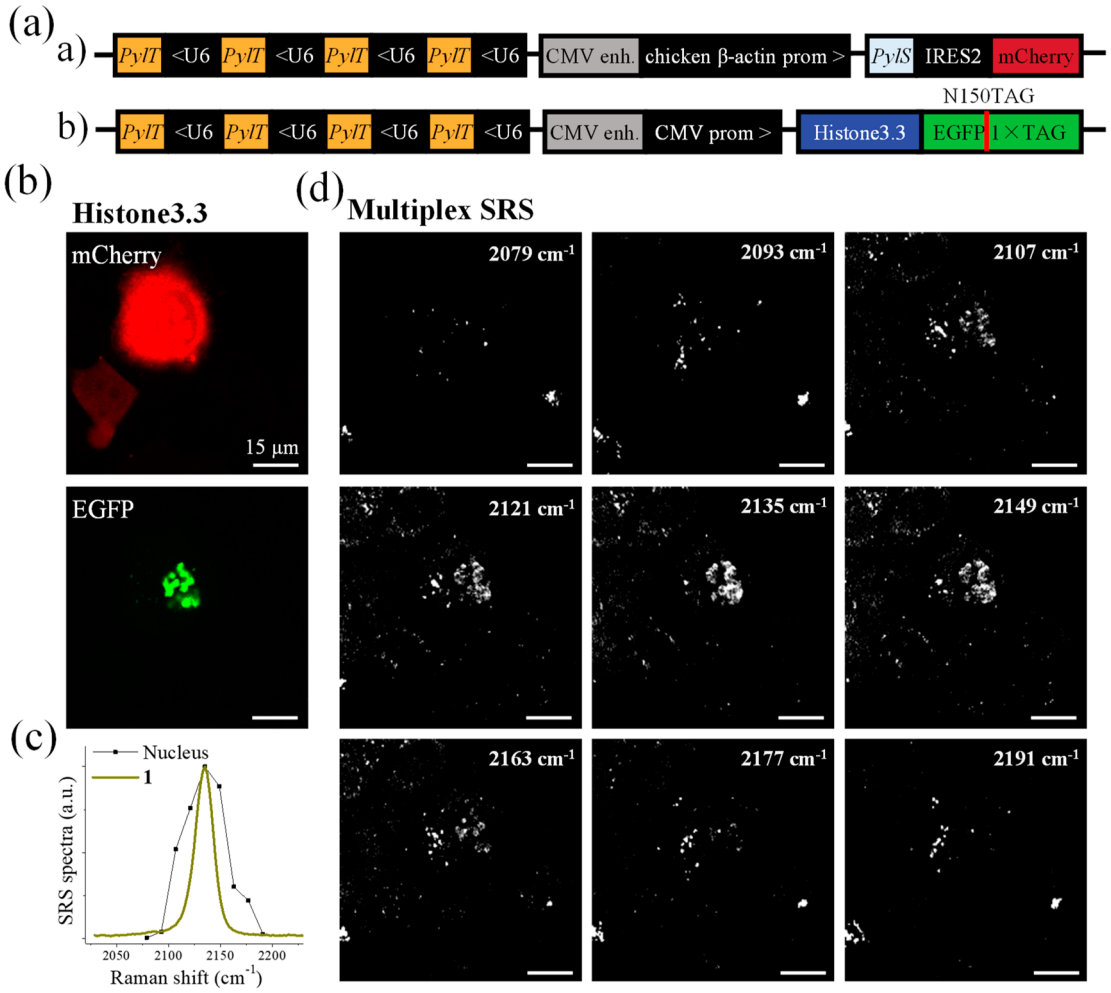


**Figure 2.** Genetic incorporation of UAA **1** in HeLa cells and SRS imaging of **1** incorporated into Histone3.3-EGFP protein. (a) Vectors used in transient transfection: a) 4×*PylT*/FLAG-*PylS*-IRES2-mCherry; b) 4×*PylT*/Histone3.3-EGFP(N150TAG). (b) TPEF images of mCherry and EGFP indicating the positions that expressed PylRS and Histone3.3-EGFP proteins, respectively. (c) SRS spectrum obtained in the location of the nucleus. SRS spectrum of **1** is shown as a reference. (d) Multiplex SRS image stack of **1** incorporated in Histone3.3-EGFP in the nucleus of a transfected cell.

image contrast of the nucleus decreased rapidly, as shown. Figure 2c illustrates the SRS spectrum acquired in the location of the nucleus (black line with dots), in which the Raman band was consistent with the SRS spectrum of UAA **1** (dark yellow). The repeated experiments are shown in Figure S3. Thus, we demonstrated that the amber-UAA-Raman tag system is capable of introducing a single-molecule Raman tag, like UAA **1**, to the desired site of the protein of interest for narrow-band molecular imaging.

*Small Phenyl Ring Enhanced Raman Tag for Sensitive Protein Imaging.* The brightness of the labels or sensitivity of the instruments is crucial for microscopic imaging. Thus the SRS signal from a single alkyne is probably too weak for any potential application. To significantly enhance the Raman signal, we designed and synthesized *N*-(3-azidopropyl)-4-(phenylbuta-1,3-diyn-1-yl)benzamide (**2**, Note S1) and then linked **1** with **2** through copper-catalyzed azide−alkyne cycloaddition (CuAAC, click chemistry, Figure 3a) in HeLa cells.[25] Despite that the newly linked Raman tag (**3**, ∼0.55 kDa, about two amino acids long) only increased about 2 times in size compared to **1**, the SRS signal increased more than 2 orders of magnitude.[20,38] As shown in Figure 3g, we measured SRS spectra of **1**, 5-ethynyl-2′-deoxyuridine (EdU), and **2** under the same experimental conditions. The Raman peak of **2** was shifted to 2225 $cm^{-1}$, and the RIE value (relative Raman intensity versus EdU) of **2** was as high as 29 due to phenyl ring enhancement,[38] which increased the SRS signal more than 2 orders of magnitude in comparison to **1** (29/0.23, ∼125 times). Meanwhile, the bandwidth (full width at half-maximum, fwhm) of **2** remained as narrow as 17.7 $cm^{-1}$, which exhibits great advantage over fluorescent labels.

To test this improvement in specific protein imaging, we introduced enhanced Raman tag **2** into the UAA system by click chemistry and performed hyperspectral SRS imaging of the Histone3.3-EGFP protein with **3**. The complete hyperspectral SRS image stack (total of 50 SRS images covering a Raman range of 2180−2280 $cm^{-1}$) is presented in Video S1. As revealed by the TPEF images of mCherry and EGFP (Figure 3b), the SRS imaging detected a strong Raman signal at 2225 $cm^{-1}$ from **3** in the nucleus of transfected cells (see the multiplex SRS image stack in Figure S4 and one of the repeated experiments in Figure S5). Figure 3c presents the raw SRS spectra collected in the locations of the nucleus, cytoplasm, and background (indicated by colored arrows in Figure 3b), while the SRS spectrum of **2** served as the internal reference (dark yellow). In the location of the nucleus, a strong



DOI: 10.1021/acs.jpclett.8b01991
J. Phys. Chem. Lett. 2018, 9, 4679−4685

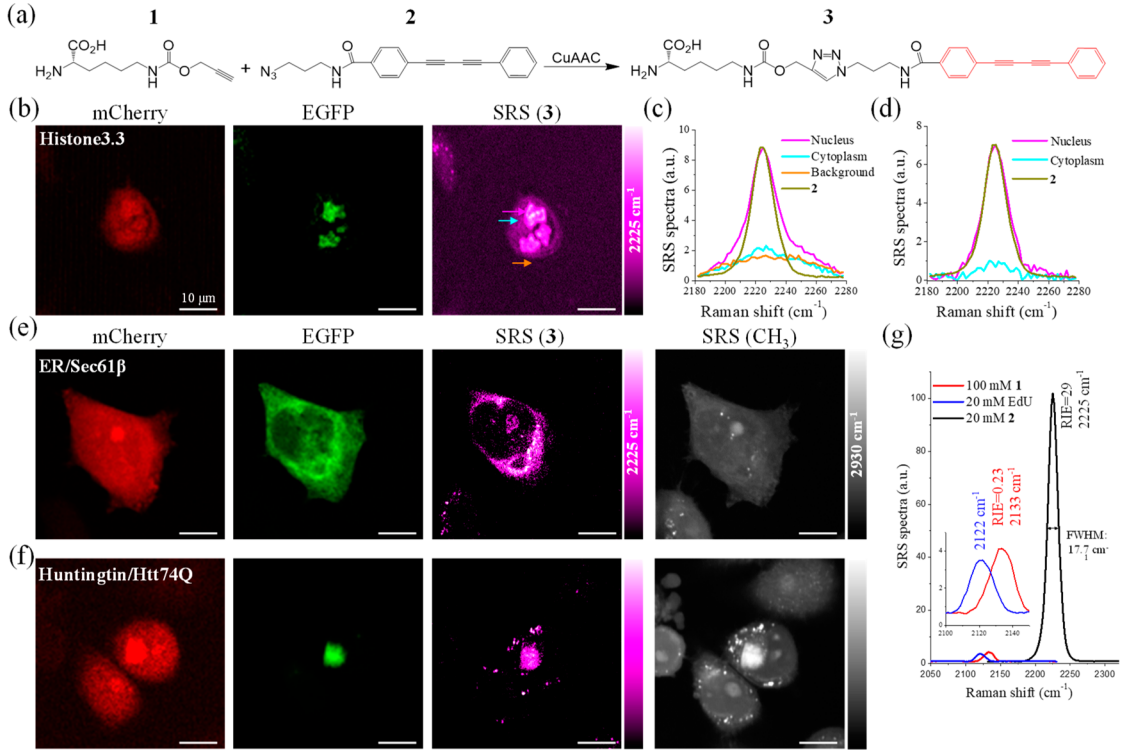


**Figure 3.** Genetic incorporation of enhanced Raman tag **2** by click chemistry. (a) Click chemistry to link **1** with azide-ended Raman tag **2**. (b) Fluorescence and hyperspectral SRS imaging of target Histone3.3-EGFP protein. TPEF images of mCherry and EGFP indicate the transfection of HeLa cell, and the SRS image at 2225 $cm^{-1}$ presents localization of the Histone3.3 protein in the nucleus after click chemistry. (c) Raw SRS spectra in the locations indicated by arrows in panel b. (d) SRS spectra after background subtraction. (e) Fluorescence and hyperspectral SRS imaging of targeted EGFP-Sec61$\beta$ protein. The SRS image of **3** presents detection of the Sec61$\beta$ protein in the ER after click chemistry, and the SRS image of $CH_3$ shows all cells in the field of view. (f) Fluorescence and hyperspectral SRS imaging of Htt74Q-EGFP protein in a Huntington diseased cell. (g) SRS spectra of 20 mM EdU, 100 mM **1**, and 20 mM **2**. The inset shows the zoomed-in spectra of **1** and EdU.

Raman peak at 2225 $cm^{-1}$ was observed, which was shifted about 90 $cm^{-1}$ from the Raman peak of alkyne (2135 $cm^{-1}$). At the cytoplasm, the SRS spectrum was featureless and similar to the background. After background subtraction (Figure 3d), the SRS spectrum in the location of the nucleus was consistent with the spectrum of **2**, suggesting that the Raman tag **2** had been successfully introduced into the Histone3.3-EGFP protein in the nucleus.

To prove that the method is applicable to any specific protein, we performed SRS imaging of Sec61$\beta$ protein in the endoplasmic reticulum (ER)[39] in HeLa cells and the Htt74Q protein in mutant huntingtin-induced cells[40] (Figure S1(4,5)). Figure 3e exhibits the corresponding mCherry and EGFP images indicating transfected cells and a target protein, the SRS image of Sec61$\beta$ protein in ER, and the SRS image showing all cells by exciting intrinsic $CH_3$ vibrations. We clearly observed that the ER target protein was distributed outside of the cell nucleus (see multiplex SRS images and spectra in Figure S6). In Figure 3f, we also conducted experiments to image the Htt74Q protein in mutant huntingtin-induced cells by SRS imaging (Figure S7). All repeated experiments are shown in Figure S8. From these observations, we confirmed that the amber-UAA-Raman tag system was capable of genetically introducing a small and strong Raman tag to a specific protein for SRS imaging.

*Direct and Sensitive SRS Imaging of Histone3.3 and Htt74Q Proteins.* To completely remove the influence of EGFP, which was initially applied as a reference for co-localization assays, we directly replaced codon K64 in *Histone3.3* with an amber codon TAG by site-directed mutagenesis.[35] Figure 4a shows the plasmid (same as in previous experiments) for expressing the PylRS/$tRNA_{CUA}$ pair (Figure 4a(a)) and the newly designed plasmid Histone3.3(K64TAG)-3×HA (Figures 4a(b) and S1(3)). The fluorescence and Western blotting experiments shown in Figure S9 indicate that EGFP was removed from the system and Histone3.3 protein was efficiently expressed. After click chemistry to introduce **2**, we performed hyperspectral SRS imaging and observed a clear spatial distribution of Histone3.3 protein in the nucleus, which was confirmed by the corresponding mCherry and $CH_3$ vibrational images (Figure 4b). Moreover, the SRS image at 2225 $cm^{-1}$ indicates that only one cell successfully expressed Histone3.3 protein. Figure 4c shows the raw SRS spectra acquired at pinpointed locations in the nucleus and cytoplasm, which displayed great spectral specificity of the UAA carried Raman tag (see the multiplex SRS in Figure S10, hyperspectral SRS image stack in Video S2, and repeated experiments in Figure S11). Furthermore, we conducted experiments to specifically image the Htt74Q protein that was highly expressed in HeLa cells due to Huntington's disease. Figure 4d,e exhibits the SRS image and spectrum of the aggregated Htt74Q protein in a HeLa cell (see the multiplex SRS image in Figure S12 and repeated experiments in Figure S13). In this case, a single amber codon TAG was inserted at the beginning of the *Htt74Q* gene (Figure S1(6)) to ensure minimal influence on protein expression and function.

We demonstrated that site-specific incorporation of UAA via the genetic code expansion technology can effectively



DOI: 10.1021/acs.jpclett.8b01991
J. Phys. Chem. Lett. 2018, 9, 4679−4685

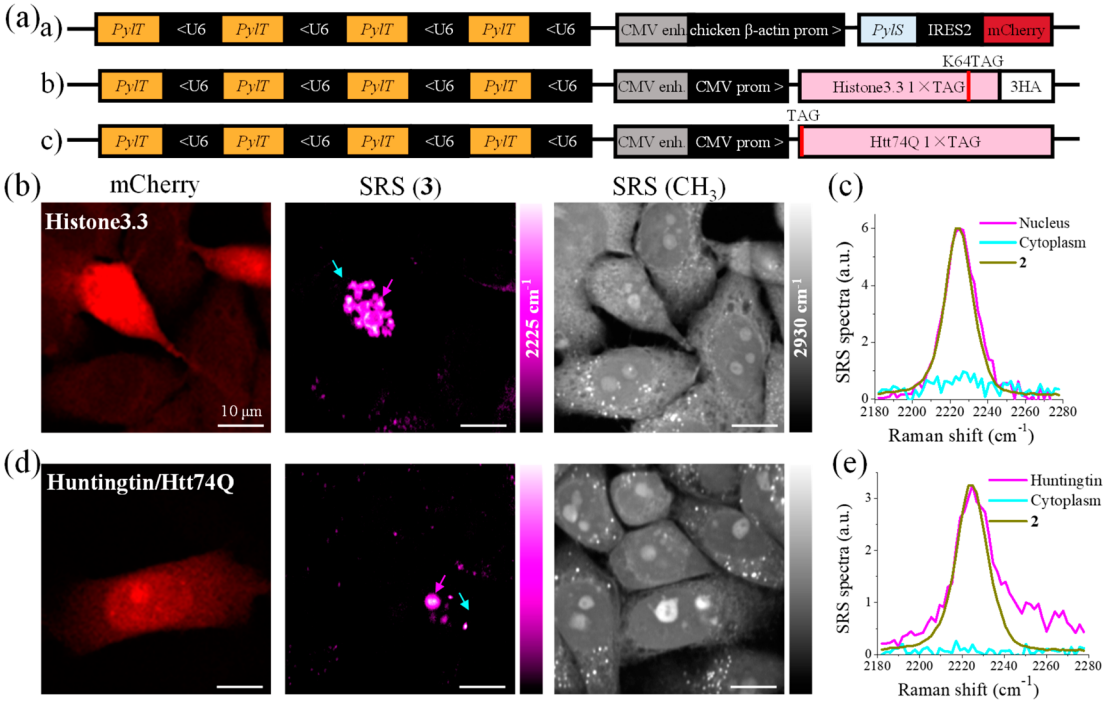


**Figure 4.** Direct incorporation of enhanced Raman tag **2** in specific proteins. (a) Vectors used for transient transfection: a) 4×*PylT*/FLAG-*PylS*-IRES2-mCherry; b) 4×*PylT*/Histone3.3(K64TAG), an amber codon TAG was used to directly replace the codon of a lysine at position 64 (K64) in *Histone3.3*; and c) 4×PylT/TAG-Htt74Q. (b) Hyperspectral SRS imaging of **3** targeted Histone3.3 protein. The TPEF image of mCherry indicates transfection of HeLa cells, the SRS image at 2225 $cm^{-1}$ presents the detection of Histone3.3 protein in the nucleus after click chemistry, and the SRS image of $CH_3$ shows all cells in the field of view. (c) SRS spectra in the locations indicated by arrows in panel b. (d) Hyperspectral SRS imaging of the Htt74Q protein in a Huntington diseased cell. (e) SRS spectra in the locations indicated by arrows in panel d.

introduce a sensitive Raman tag as small as 0.5 kDa to specific proteins for molecular SRS imaging. To prove our concept, we genetically incorporated an alkyne and further a small phenyl ring enhanced Raman tag to Histone3.3, Sec61$\beta$, and Htt74Q proteins with molecular precision in HeLa cells and performed hyperspectral SRS imaging of the target protein. For future applications, it is straightforward to achieve live cell imaging of other intracellular proteins by copper-free click chemistry.[12,41] On the basis of the excellent property of Raman tags, supermultiplex Raman imaging of multiple proteins can be further realized by applying powerful quadruplet codons,[42] unnatural codons,[43] and other advanced genetic approaches to expand new blank codons.

## ■ ASSOCIATED CONTENT

### Supporting Information

The Supporting Information is available free of charge on the ACS Publications website at DOI: 10.1021/acs.jpclett.8b01991.

Details of the hyperspectral SRS microscope setup; materials and experimental details for fluorescence, Western blotting, and SRS; additional data for TPEF and SRS images, synthesis of **2**; and the sequences of plasmids (PDF)

Complete hyperspectral SRS image stack of Histone3.3-EGFP protein (AVI)

Complete hyperspectral SRS image stack of Histone3.3 protein (AVI)

### Accession Codes

The data that support the findings of this study are available from the corresponding authors upon request.

## ■ AUTHOR INFORMATION


### Corresponding Author

*E-mail: p_wang@hust.edu.cn.

### ORCID

Jing Zhang: 0000-0003-0328-3600
Shuai Yan: 0000-0002-9083-7749
Zhiyong He: 0000-0001-7976-9928
Xiang Zhou: 0000-0002-1829-9368
Ping Wang: 0000-0002-5168-6829


### Author Contributions

#J.Z., S.Y., Z.H., and C.D. contributed equally.

### Notes

The authors declare no competing financial interest.

## ■ ACKNOWLEDGMENTS

We thank Fan Jia and Fuqiang Xu for providing the p357 vector, Xiang Yu and Zhihong Zhang for providing the pEGFP-N1 vector, and Yali Bi for helpful suggestions on the manuscript. We thank the Analytical & Testing center of HUST for measurements of Raman spectra. P.W. acknowledges support from the National Key Research and Development Program of China (2016YFA0201403), the National Natural Science Foundation of China (61675075), the Science Fund for Creative Research Group of China (61721092), and the Chinese Recruitment Program of Global Experts and Director Fund of the Wuhan National Laboratory for Optoelectronics.



DOI: 10.1021/acs.jpclett.8b01991
J. Phys. Chem. Lett. 2018, 9, 4679−4685

## REFERENCES


(1) Tsien, R. Y. The green fluorescent protein. *Annu. Rev. Biochem.* **1998**, *67*, 509−544.
(2) Hoffmann, C.; Gaietta, G.; Bunemann, M.; Adams, S. R.; Oberdorff-Maass, S.; Behr, B.; Vilardaga, J. P.; Tsien, R. Y.; Ellisman, M. H.; Lohse, M. J. A FlAsH-based FRET approach to determine G protein-coupled receptor activation in living cells. *Nat. Methods* **2005**, *2*, 171−176.
(3) Vilardaga, J. P.; Bunemann, M.; Krasel, C.; Castro, M.; Lohse, M. J. Measurement of the millisecond activation switch of G protein-coupled receptors in living cells. *Nat. Biotechnol.* **2003**, *21*, 807−812.
(4) Stadler, C.; Rexhepaj, E.; Singan, V. R.; Murphy, R. F.; Pepperkok, R.; Uhlen, M.; Simpson, J. C.; Lundberg, E. Immunofluorescence and fluorescent-protein tagging show high correlation for protein localization in mammalian cells. *Nat. Methods* **2013**, *10*, 315−323.
(5) Niehorster, T.; Loschberger, A.; Gregor, I.; Kramer, B.; Rahn, H. J.; Patting, M.; Koberling, F.; Enderlein, J.; Sauer, M. Multi-target spectrally resolved fluorescence lifetime imaging microscopy. *Nat. Methods* **2016**, *13*, 257−262.
(6) Hao, B.; Gong, W.; Ferguson, T. K.; James, C. M.; Krzycki, J. A.; Chan, M. K. A new UAG-encoded residue in the structure of a methanogen methyltransferase. *Science* **2002**, *296*, 1462−1466.
(7) Srinivasan, G.; James, C. M.; Krzycki, J. A. Pyrrolysine encoded by UAG in Archaea: charging of a UAG-decoding specialized tRNA. *Science* **2002**, *296*, 1459−1462.
(8) Fekner, T.; Li, X.; Lee, M. M.; Chan, M. K. A pyrrolysine analogue for protein click chemistry. *Angew. Chem., Int. Ed.* **2009**, *48*, 1633−1635.
(9) Summerer, D.; Chen, S.; Wu, N.; Deiters, A.; Chin, J. W.; Schultz, P. G. A genetically encoded fluorescent amino acid. *Proc. Natl. Acad. Sci. U. S. A.* **2006**, *103*, 9785−9789.
(10) Wang, J.; Xie, J.; Schultz, P. G. A genetically encoded fluorescent amino acid. *J. Am. Chem. Soc.* **2006**, *128*, 8738−8739.
(11) Marek, P.; Gupta, R.; Raleigh, D. P. The fluorescent amino acid p-cyanophenylalanine provides an intrinsic probe of amyloid formation. *ChemBioChem* **2008**, *9*, 1372−1374.
(12) Peng, T.; Hang, H. C. Site-specific bioorthogonal labeling for fluorescence imaging of intracellular proteins in living cells. *J. Am. Chem. Soc.* **2016**, *138*, 14423−14433.
(13) Adams, S. R.; Campbell, R. E.; Gross, L. A.; Martin, B. R.; Walkup, G. K.; Yao, Y.; Llopis, J.; Tsien, R. Y. New biarsenical ligands and tetracysteine motifs for protein labeling in vitro and in vivo: synthesis and biological applications. *J. Am. Chem. Soc.* **2002**, *124*, 6063−6076.
(14) Georgieva, M. V.; Yahya, G.; Codo, L.; Ortiz, R.; Teixido, L.; Claros, J.; Jara, R.; Jara, M.; Iborra, A.; Gelpi, J. L.; et al. Inntags: small self-structured epitopes for innocuous protein tagging. *Nat. Methods* **2015**, *12*, 955−958.
(15) Luo, X.; Zambaldo, C.; Liu, T.; Zhang, Y.; Xuan, W.; Wang, C.; Reed, S. A.; Yang, P. Y.; Wang, R. E.; Javahishvili, T.; et al. Recombinant thiopeptides containing noncanonical amino acids. *Proc. Natl. Acad. Sci. U. S. A.* **2016**, *113*, 3615−3620.
(16) Nikic, I.; Plass, T.; Schraidt, O.; Szymanski, J.; Briggs, J. A.; Schultz, C.; Lemke, E. A. Minimal tags for rapid dual-color live-cell labeling and super-resolution microscopy. *Angew. Chem., Int. Ed.* **2014**, *53*, 2245−2249.
(17) Grammel, M.; Hang, H. C. Chemical reporters for biological discovery. *Nat. Chem. Biol.* **2013**, *9*, 475−484.
(18) Zhao, Z.; Shen, Y.; Hu, F.; Min, W. Applications of vibrational tags in biological imaging by Raman microscopy. *Analyst* **2017**, *142*, 4018−4029.
(19) Wei, L.; Chen, Z.; Shi, L.; Long, R.; Anzalone, A. V.; Zhang, L.; Hu, F.; Yuste, R.; Cornish, V. W.; Min, W. Super-multiplex vibrational imaging. *Nature* **2017**, *544*, 465−470.
(20) Hu, F.; Zeng, C.; Long, R.; Miao, Y.; Wei, L.; Xu, Q.; Min, W. Supermultiplexed optical imaging and barcoding with engineered polyynes. *Nat. Methods* **2018**, *15*, 194−200.
(21) Freudiger, C. W.; Min, W.; Saar, B. G.; Lu, S.; Holtom, G. R.; He, C.; Tsai, J. C.; Kang, J. X.; Xie, X. S. Label-free biomedical imaging with high sensitivity by stimulated Raman scattering microscopy. *Science* **2008**, *322*, 1857−1861.
(22) Yang, Y.; Chen, L.; Ji, M. Stimulated Raman scattering microscopy for rapid brain tumor histology. *J. Innovative Opt. Health Sci.* **2017**, *10*, 1730010.
(23) Nguyen, D. P.; Lusic, H.; Neumann, H.; Kapadnis, P. B.; Deiters, A.; Chin, J. W. Genetic encoding and labeling of aliphatic azides and alkynes in recombinant proteins via a pyrrolysyl-tRNA synthetase/$tRNA_{CUA}$ pair and click chemistry. *J. Am. Chem. Soc.* **2009**, *131*, 8720−8721.
(24) Hancock, S. M.; Uprety, R.; Deiters, A.; Chin, J. W. Expanding the genetic code of yeast for incorporation of diverse unnatural amino acids via a pyrrolysyl-tRNA synthetase/tRNA pair. *J. Am. Chem. Soc.* **2010**, *132*, 14819−14824.
(25) Lang, K.; Chin, J. W. Cellular incorporation of unnatural amino acids and bioorthogonal labeling of proteins. *Chem. Rev.* **2014**, *114*, 4764−4806.
(26) Greiss, S.; Chin, J. W. Expanding the genetic code of an animal. *J. Am. Chem. Soc.* **2011**, *133*, 14196−14199.
(27) Krogager, T. P.; Ernst, R. J.; Elliott, T. S.; Calo, L.; Beranek, V.; Ciabatti, E.; Spillantini, M. G.; Tripodi, M.; Hastings, M. H. Labeling and identifying cell-specific proteomes in the mouse brain. *Nat. Biotechnol.* **2017**, *36*, 156−159.
(28) Wang, L.; Xie, J.; Schultz, P. G. Expanding the genetic code. *Annu. Rev. Biophys. Biomol. Struct.* **2006**, *35*, 225−249.
(29) Liu, C. C.; Schultz, P. G. Adding new chemistries to the genetic code. *Annu. Rev. Biochem.* **2010**, *79*, 413−444.
(30) Chin, J. W. Expanding and reprogramming the genetic code of cells and animals. *Annu. Rev. Biochem.* **2014**, *83*, 379−408.
(31) Wei, L.; Hu, F.; Shen, Y.; Chen, Z.; Yu, Y.; Lin, C. C.; Wang, M. C.; Min, W. Live-cell imaging of alkyne-tagged small biomolecules by stimulated Raman scattering. *Nat. Methods* **2014**, *11*, 410−412.
(32) Hong, S.; Chen, T.; Zhu, Y.; Li, A.; Huang, Y.; Chen, X. Live-cell stimulated Raman scattering imaging of alkyne-tagged biomolecules. *Angew. Chem., Int. Ed.* **2014**, *53*, 5827−5831.
(33) Li, S.; Chen, T.; Wang, Y.; Liu, L.; Lv, F.; Li, Z.; Huang, Y.; Schanze, K. S.; Wang, S. Conjugated polymer with intrinsic alkyne units for synergistically enhanced Raman imaging in living cells. *Angew. Chem., Int. Ed.* **2017**, *56*, 13455−13458.
(34) Schmied, W. H.; Elsasser, S. J.; Uttamapinant, C.; Chin, J. W. Efficient multisite unnatural amino acid incorporation in mammalian cells via optimized pyrrolysyl tRNA synthetase/tRNA expression and engineered eRF1. *J. Am. Chem. Soc.* **2014**, *136*, 15577−15583.
(35) Elsässer, S. J.; Ernst, R. J.; Walker, O. S.; Chin, J. W. Genetic code expansion in stable cell lines enables encoded chromatin modification. *Nat. Methods* **2016**, *13*, 158−164.
(36) Lang, K.; Davis, L.; Wallace, S.; Mahesh, M.; Cox, D. J.; Blackman, M. L.; Fox, J. M.; Chin, J. W. Genetic encoding of bicyclononynes and trans-cyclooctenes for site-specific protein labeling in vitro and in live mammalian cells via rapid fluorogenic Diels-Alder reactions. *J. Am. Chem. Soc.* **2012**, *134*, 10317−10320.
(37) Bazewicz, C. G.; Lipkin, J. S.; Smith, E. E.; Liskov, M. T.; Brewer, S. H. Expanding the utility of 4-cyano-L-phenylalanine as a vibrational reporter of protein environments. *J. Phys. Chem. B* **2012**, *116*, 10824−10831.
(38) Yamakoshi, H.; Dodo, K.; Palonpon, A.; Ando, J.; Fujita, K.; Kawata, S.; Sodeoka, M. Alkyne-tag Raman imaging for visualization of mobile small molecules in live cells. *J. Am. Chem. Soc.* **2012**, *134*, 20681−20689.
(39) Zhu, Y.; Zhang, G.; Lin, S.; Shi, J.; Zhang, H.; Hu, J. Sec61$\beta$ facilitates the maintenance of endoplasmic reticulum homeostasis by associating microtubules. *Protein Cell* **2018**, *9*, 616−628.
(40) Miki, Y.; Tanji, K.; Mori, F.; Wakabayashi, K. Sigma-1 receptor is involved in degradation of intranuclear inclusions in a cellular model of Huntington's disease. *Neurobiol. Dis.* **2015**, *74*, 25−31.



DOI: 10.1021/acs.jpclett.8b01991
*J. Phys. Chem. Lett.* 2018, 9, 4679−4685

(41) Plass, T.; Milles, S.; Koehler, C.; Schultz, C.; Lemke, E. A. Genetically encoded copper-free click chemistry. *Angew. Chem., Int. Ed.* **2011**, *50*, 3878−3881.
(42) Neumann, H.; Wang, K. H.; Davis, L.; Garcia-Alai, M.; Chin, J. W. Encoding multiple unnatural amino acids via evolution of a quadruplet-decoding ribosome. *Nature* **2010**, *464*, 441−444.
(43) Zhang, Y.; Ptacin, J. L.; Fischer, E. C.; Aerni, H. R.; Caffaro, C. E.; San Jose, K.; Feldman, A. W.; Turner, C. R.; Romesberg, F. E. A semi-synthetic organism that stores and retrieves increased genetic information. *Nature* **2017**, *551*, 644−647.



DOI: 10.1021/acs.jpclett.8b01991
*J. Phys. Chem. Lett.* 2018, 9, 4679−4685